CONSISTENT ESTIMATION OF BUILDING PARAMETERS CONSIDERING GEOMETRIC REGULARITIES BY SOFT CONSTRAINTS

Franz Rottensteiner

Institute of Photogrammetry and Remote Sensing, Vienna University of Technology,
Gußhausstraße 27-29, A-1040 Vienna, Austria - fr@ipf.tuwien.ac.at

Cooperative Research Centre for Spatial Information,
723 Swanston Street, The University of Melbourne, VIC 3010, Australia – franzr@unimelb.edu.au

Commission III, WG III/4

KEY WORDS: Building Reconstruction, Parameter Estimation, Constraints

ABSTRACT:

This paper describes a model for the consistent estimation of building parameters that is a part of a method for automatic building reconstruction from airborne laser scanner (ALS) data. The adjustment model considers the building topology by GESTALT observations, i.e. observations of points being situated in planes. Geometric regularities are considered by "soft constraints" linking neighbouring vertices or planes. Robust estimation can be used to eliminate false hypotheses about such geometric regularities. Sensor data provide the observations to determine the parameters of the building planes. The adjustment model can handle a variety of sensor data and is shown to be also applicable for semi-automatic building reconstruction from image and/or ALS data. A test project is presented in order to evaluate the accuracy that can be achieved using our technique for building reconstruction from ALS data, along with the improvement caused by adjustment and regularisation. The planimetric accuracy of the building walls is in the range of or better than the ALS point distance, whereas the height accuracy is in the range of a few centimetres. Regularisation was found to improve the planimetric accuracy by 5- 45%.

1. INTRODUCTION

The shapes of buildings and other man-made objects, despite being very complex in realistic scenes, are often characterised by certain geometrical regularities. At a level of detail typical for topographic mapping (mapping scales 1:500 to 1:1000) most buildings can be modelled by polyhedrons. This implies that all vertices belonging to a face must be situated on a plane in object space. Apart from that, other geometrical regularities include perpendicular walls, horizontal roof edges, or symmetry between roof faces.

It is the goal of automatic building reconstruction to generate 3D building models from sensor data in previously detected regions of interest. In this context, model regularisation by considering geometric constraints is essential for achieving high quality building models. Besides resulting in a more regular visual appearance, considering geometric regularities helps to improve the geometric accuracy of the models, especially if the sensor geometry is weak. There are two general strategies for building reconstruction, differing in the way buildings are represented in the reconstruction process and thus also in the way geometric regularities are considered. The first strategy is based on a bottom-up process. The sensor data are segmented in order to obtain 3D features such as edges and planes. These features are combined to obtain a polyhedral model, e.g. (Rottensteiner et al., 2005). Alternatively, buildings can be reconstructed by parametric primitives in a top-down process, e.g. (Brenner, 2000). In the first case, assumptions on geometric regularities may or may not be used in order to select the 3D features and group them; they can and should be considered as additional information in a final parameter estimation process yielding consistent and regularised building models. In the second case, assumptions about regularities, e.g. rectangular footprints, are an implicit part of the description of the primitives. Using parametric primitives reduces the level of detail that can be achieved as the number of primitives is usually small and most have a rectangular footprint. This can be avoided by using "adaptive primitives" (Rottensteiner & Schulze, 2003), i.e. primitives having an adaptive parameterisation. However, the bottom-up strategy seems to be more flexible with respect to handling geometric regularities. They are not an implicit part of the building model, but rather are added as additional information to the estimation of the building parameters and thus only have to be considered where enough evidence is found in the data. From the point of view of parameter estimation, this can be handled in two ways. First, geometric regularities can be considered in the adjustment by constraint equations. This strategy will result in models precisely fulfilling these "hard" constraints. Brenner (2005) has given an overview about the ways such constraints can be handled in object modelling. The alternative is to add "soft constraints", i.e. direct observations for entities describing a geometric regularity, to the adjustment of the sensor-based observations. In this case, the constraints will not be fulfilled exactly, but there will be residuals to the observations. The degree to which the constraints are fulfilled depends on the stochastic model. Using the second strategy, robust estimation techniques can be applied to the soft constraints to determine whether a hypothesis about a geometric regularity fits to the sensor data or not.

Vosselman (1999) proposed an algorithm for building reconstruction from airborne laser scanner (ALS) data that determined building outlines under the assumption of all neighbouring walls intersecting at right angles. He addressed

the necessity of adding constraints to the estimation of the model parameters without doing so himself. Vögtle and Steinle (2000) reconstruct buildings from ALS and spectral data. The coordinates of their building vertices are estimated by local adjustment only, and no geometric regularities are considered. Alharty and Bethel (2004) describe two methods for roof outline detection. The first method relies on the existence of a dominant roof direction and the neighbouring walls being orthogonal. The second does not require such assumptions, but no overall adjustment is carried out, and no geometric regularities are considered. Ameri (2000) describes a general adjustment model for building reconstruction from image data. Geometric constraints are considered. For instance, for two orthogonal building edges a direct observation of the inner product of the directional vectors is introduced. The weighting of such an algebraic observation seems to be somewhat critical. A method for fitting building models to multiple aerial images using "hard" constraints was presented in (Vallet & Taillandier, 2005). McGlone (1996) describes the mathematical basis for handling geometrical constraints both as ("hard") condition equations and as "soft" constraints, using this basis for improving the results of multiple-image point matching under the assumption of certain object regularities.

In (Rottensteiner et al., 2005) we have presented a method for automatic building reconstruction from ALS data that is based on the detection and combination of roof planes. The final step of building reconstruction is an overall adjustment of all observations to determine the model parameters consistently. The adjustment model was originally presented in (Rottensteiner, 2003), but implemented only recently. It is the first goal of this paper to present this adjustment model in its improved and revised form and to show how it can be used as a tool for consistent estimation of building parameters for different types of available sensor data. Special emphasis is laid on the way geometric regularities can be considered. The second goal of this paper is to evaluate the results of building reconstruction from ALS data by comparing automatically derived building models to reference data. This comparison should also show how effective the overall adjustment is in improving the geometric quality of building models.

2. WORKFLOW FOR BUILDING RECONSTRUCTION

Our algorithm for building reconstruction requires ALS points and a coarse approximation of the building outlines. The ALS data are sampled into a Digital Surface Model (DSM) in the form of a regular grid of width Δ by linear prediction. The work flow consists of three steps (Rottensteiner et al., 2005):

1. **Detection of roof planes** based on a segmentation of the DSM. These planes are expanded by region growing.
2. **Grouping of roof planes and roof plane delineation:** Co-planar roof planes are merged, and hypotheses for intersection lines and/or step edges are created based on an analysis of the neighbourhood relations of the roof planes.
3. **Consistent estimation of the building parameters** to improve these parameters using all available sensor data and considering geometric constraints.

In step 2, the boundary polygons of the roof planes are determined as a combination of roof plane intersections and step edges, the step edges being located in the DSM by an edge extraction technique taking into account specific information about buildings. Decisions in the determination of the shapes of the roof polygons are based on hypotheses tests and robust estimation. We use the concept of uncertain projective geometry (Heuel, 2004) for consistent modelling of the stochastic properties of all geometric entities. In this paper, we will focus on the final step of the reconstruction process.

3. THE ADJUSTMENT MODEL

The adjustment problem we want to solve can be described as follows. We assume to have given a polyhedral building model in boundary representation (B-rep). The model consists of planar faces, loops, edges, and vertices. Each edge is the intersection of two neighbouring faces, and each vertex is the intersection of at least three planes of the model. All vertices belonging to the boundary of a face have to lie in the face's plane. The faces of the model are labelled as being a roof face, a wall, or the floor. Walls are modelled to be strictly vertical. The topology of the model and some meaningful initial values for its parameters are assumed to be known. The initial model can be the outcome of the bottom-up strategy for building reconstruction (cf. section 2). In this case it is an approximate version of the final model, and its initial parameters are already derived in some way from the sensor data. The coarse model has to be analysed for geometric regularities, which can be done automatically or based on the interaction of a human operator, and the model parameters have to be estimated. For that purpose, we use five categories of observations:

1. Observations representing the topology of the model
2. Observations corresponding to geometric regularities
3. Sensor and sensor-derived observations
4. Observations linking the sensor observations to the model
5. Direct observations for unknowns to avoid singularities.

They are used to determine four categories of unknowns:

1. The co-ordinates of the model vertices
2. The parameters of the model planes
3. Transformation parameters, e.g. the unknown angle for each pair of perpendicular walls (cf. section 3.2)
4. Additional unknowns, e.g. unknown object co-ordinates for each ALS point (cf. section 3.3.2).

Our method for handling the model topology and geometric regularities is independent not only from the types of sensor data that are used, but also from the way in which the original model was created. The adjustment model is based on the program ORIENT for hybrid photogrammetric adjustment, especially on its concept of handling object space constraints by "GESTALT" observations (Kager, 2000).

3.1 Observations Representing Model Topology

It is the idea of our method to find a mapping between the B-rep of the polyhedral model and a system of GESTALT observations representing the model topology in adjustment. GESTALT observations are observations of a point $\mathbf{P}$ being situated on a polynomial surface (Kager, 2000). The polynomial is parameterised in an observation co-ordinate system (u, v, w) related to the object co-ordinate system by a shift $\mathbf{P_0}$ and three rotations $\boldsymbol{\Theta} = (\varpi, \phi, \kappa)^T$. The actual observation is $\mathbf{P}$'s distance from the surface which has to be 0. Using $(u_R, v_R, w_R)^T = \mathbf{R}^T(\boldsymbol{\Theta}) \cdot (\mathbf{P} - \mathbf{P_0})$, with $\mathbf{R}^T(\boldsymbol{\Theta})$ being a transposed rotational matrix parameterised by $\boldsymbol{\Theta}$, and restricting ourselves to vertical planes for walls and tilted planes for roofs, there are three possible formulations of GESTALT observation equations:

$$
\begin{aligned}
r_u &= \frac{m_u \cdot u_R + a_{00} + a_{01} \cdot m_v \cdot v_R}{\sqrt{1 + a_{01}^2}} \\
r_v &= \frac{m_v \cdot v_R + b_{00} + b_{10} \cdot m_u \cdot u_R}{\sqrt{1 + b_{10}^2}} \\
r_w &= \frac{m_w \cdot w_R + c_{00} + c_{10} \cdot (m_u \cdot u_R) + c_{01} \cdot (m_v \cdot v_R)}{\sqrt{1 + c_{10}^2 + c_{01}^2}}
\end{aligned} \qquad (1)
$$

In equation 1, r_i are the corrections of the fictitious observations of co-ordinate i and $m_i \in \{-1, 1\}$ are mirror coefficients. An application is free to decide which of the parameters (**P**, $\mathbf{P_0}$, **Θ**, a_{jk}, b_{ik}, c_{ij}) are to be determined in adjustment and how to parameterise a surface. In addition, different GESTALTs can refer to identical transformation or surface parameters, which will be used to handle geometric regularities (cf. section 3.2). Here, we declare the rotations to be 0 and constant. $\mathbf{P_0}$ is a point situated inside the building and constant. For each face of the B-rep of the building model, we define a set of GESTALT observations, taking one of the first two equations 1 for walls and the third one for roofs. The unknowns to be determined are the object co-ordinates of each vertex **P** and the plane parameters (a_{jk}, b_{ik}, c_{ij}). As each vertex is neighboured by at least three faces, the co-ordinates of the vertices are determined from these GESTALT observations and thus need not be observed directly in the sensor data. Further, these observations link the vertex co-ordinates to the surface parameters and thus represent the building topology in the adjustment. They do already enforce geometric constraints by modelling walls as being strictly vertical and by declaring all vertices of a face to lie in the same plane. The stochastic model of these GESTALT observations is described by the a priori standard deviation σ_T of the fictitious distance between a point and the plane.

3.2 Observations Representing Geometric Regularities

Geometric regularities are considered by additional GESTALT equations, taking advantage of specific definitions of the observation co-ordinate system and specific parameterisations of the planes. Geometric regularities can occur between two planes or between two vertices of the model. In the current implementation, we restrict ourselves to regularities involving planes or vertices being neighbours of one edge. In all cases, the observation co-ordinate system is centred in one vertex $\mathbf{P_1}$ of that edge and the w-axis is vertical, thus $\varpi = \phi = 0 = const$. Four types of geometric regularities are considered (Figure 1). The first type, a horizontal roof edge, involves the edge's end points: Its two vertices $\mathbf{P_1}$ and $\mathbf{P_2}$ must have identical heights. The two points are declared to be in a horizontal plane ε_h that is identical to the (u,v) – plane of the observation co-ordinate system. One observation is inserted for $\mathbf{P_2}$: $r_w = w_R = Z_2 - Z_1$.

The other cases involve the two neighbouring planes of an edge. One of the axes of the observation coordinate system is defined to be the intersection of these two planes ε_1 and ε_2. There is one additional unknown rotational angle κ describing the direction of the u-axis. For each vertex $\mathbf{P}_i$ of the planes, GESTALT observations are added for ε_1 or ε_2. For the edge's second vertex $\mathbf{P}_2$ two observations (one per plane) are added. The GESTALT observations for ε_1 and ε_2 are parameterised in a specific way:

- The edge is the intersection of two horizontal and symmetric roof planes ε_1 and ε_2. There is only one tilt parameter c^1_{01}. Symmetry is enforced by selecting $m_v = -1$ for ε_2:

$$
\varepsilon_1 : r_w = \frac{w_R + c^1_{01} \cdot v_R}{\sqrt{1 + \left(c^1_{01}\right)^2}}; \qquad \varepsilon_2 : r_w = \frac{w_R - c^1_{01} \cdot v_R}{\sqrt{1 + \left(c^1_{01}\right)^2}} \qquad (2)
$$

- The edge is the intersection of two perpendicular walls: ε_1: $r_u = u_R$, ε_2: $r_v = v_R$. There is no additional surface parameter to be determined.
- Two walls are identical and the edge does not really exist in the object: ε_1: $r_v = v_R$, ε_2: $r_v = v_R$. There is no additional surface parameter. $\mathbf{P}_1$ and/or $\mathbf{P}_2$ might become undetermined, so that direct observations for one of the co-ordinates of these vertices have to be generated.

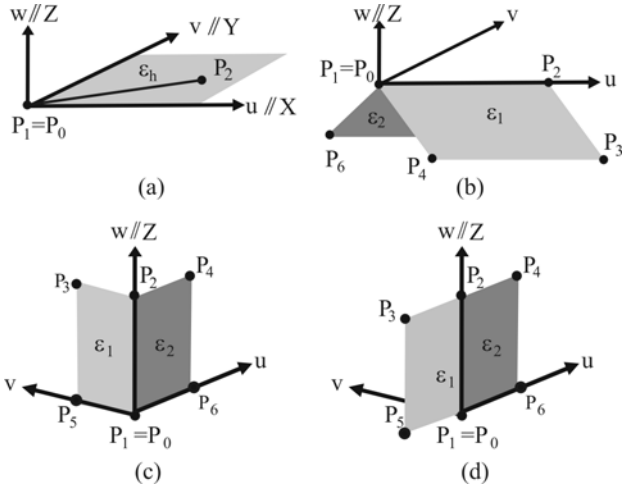

Figure 1. (a) Horizontal edge; (b) horizontal and symmetric edge; (c) perpendicular walls; (d) Identical walls.

The stochastic model of these GESTALT observations is described by their a priori standard deviations σ_C. The "soft constraints" thus modelled will only be fulfilled up to a degree depending on σ_C. The GESTALT observations corresponding to the geometrical constraints can be subject to robust estimation for gross error detection. If the sensor observations contradict the constraints, the respective GESTALT observations should receive large residuals, which can be used to modulate the weights in an iterative robust estimation procedure (Kager, 2000). Thus, if the GESTALT observations describing a geometric constraint are eliminated in adjustment, this means that the hypothesis about a constraint was wrong.

Whether or not a hypothesis about a constraint is introduced can be decided in several ways. For instance, the coarse model can be analysed whether the angles between neighbouring walls differ from 90° by less than a threshold ε_α, and a constraint about perpendicular walls can be inserted if this is the case. More sophisticated methods can take into account the stochastic properties of the coarse model. In a semi-automatic working environment, geometric constraints can be inserted (and enforced) by the user. The principle can be expanded to the definition of parametric primitives by generating more complex systems of constraints between the planes of a building (Rottensteiner & Schulze, 2003).

3.3 Sensor Observations and Observations Linking the Sensor Data to the Model

The observations described so far link the plane parameters to the vertices or to the parameters of other planes. In order to determine the surface parameters, observations derived from the sensor data are necessary. ORIENT can handle a large variety

of sensor models. Any of these sensors or any combination of them can be used in adjustment. Here we will restrict ourselves to image and ALS data.

3.3.1 Image co-ordinates: Points measured in images are related to object space by the perspective equations. We assume the orientation parameters of the images to be known and constant. An observed image point has to be assigned to an entity of the object model to contribute to the determination of the model parameters. Two cases can be distinguished. First, an image point can be assigned to a building vertex, which yields two perspective observation equations for that vertex. Second, the image point can be assigned to a model edge. As such a point is not a part of the model, its object co-ordinates have to be determined as additional unknowns; however, each point assigned to an object edge yields four additional observations: its two image co-ordinates and two GESTALT observations (one for each object plane intersecting at the object edge). The stochastic model of an image co-ordinate is described by its standard deviation σ_I. Depending on the way the image points were determined, σ_I can describe the accuracy of manual measurement, or it can be the result of a feature extraction process.

3.3.2 ALS data: ALS points give support to the determination of the roof plane parameters. As an ALS point is not a part of the model, its object co-ordinates have to be determined as unknowns. Each ALS point gives four observations, namely its three co-ordinates and one GESTALT observation for the roof plane the point is assigned to. As the walls only receive few laser hits, their parameters have to be determined from other observations. Walls correspond to sections of step edges in the DSM (Rottensteiner et al., 2005). Each step edge section is derived from "edge points" in the DSM (e.g. points of maximum height gradient). In order to determine the walls, these edge points have to be used as observations in a way similar to the original ALS points: Each edge point gives three observations (its X and Y co-ordinates and 1 GESTALT), but two additional unknowns (again X and Y). The ALS observations can be modelled in two different ways: They can be introduced as "control point" observations, i.e. as direct observations for the object co-ordinates, or they can be introduced as "model points". In the latter case, the ALS points are linked to the object co-ordinate system by a rigid motion, and the six parameters of that rigid motion are estimated in the adjustment. Using this variant, local shifts and rotations of the ALS co-ordinate system with respect to the object co-ordinate system that might be the result of systematic GPS and INS errors of the ALS system can be compensated. This only makes sense if additional data, e.g. aerial images, are available. Otherwise, the ALS and the object co-ordinate systems are assumed to be identical. The stochastic model of an ALS point is described by two standard deviations: σ_{XY} for its planimetric co-ordinates and σ_Z for its height. The edge point co-ordinates are introduced with a standard deviation σ_E.

3.4 Overall Adjustment

All observations are used in an overall adjustment process. The weights of the observations are determined from their a priori standard deviations. Correlations between the observations (e.g. between the x and y image co-ordinates of an image point) are not considered. Robust estimation is carried out by iteratively re-weighting the observations depending on their normalised residuals in the previous adjustment (Kager, 2000). The re-weighting scheme is only applied to the sensor observations and to the observations modelling geometric constraints, in order to eliminate gross observation errors and wrong hypotheses about geometric regularities. The surface parameters and the vertex co-ordinates determined in the adjustment are used to derive the final building model.

4. EVALUATION

4.1 The Test Data

For our test, we selected 8 buildings of different size and complexity out of a larger test area in Fairfield (NSW). They were chosen to highlight the method's potential to handle buildings of both regular and irregular shapes. Both ALS and image data were available for that test site. The ALS data were captured using an Optech ALTM 3025 laser scanner with a nominal average point distance of 1.25 m. As our test buildings were at the edge of a swath, there was a relatively irregular point density, with point distances of about 0.5 m in flight direction and 1.5 - 2 m across flight direction. The aerial images were a stereo pair taken at a scale of 1:11000 (focal length f = 30 cm). They were scanned at a resolution 15 μm, which corresponds to a ground sampling distance of 0.17 m.

4.2 Generating Reference Data

The aerial images were used to determine the reference data for the test. In a semi-automatic working environment, the roof polygons were digitised in the images and hypotheses about geometric regularities were introduced by the human operator. The adjustment model described in section 3 was used to determine the parameters of the reference buildings, taking into account the GESTALT observations, the image co-ordinates of the building vertices, and ALS points to improve the height accuracy of the reference models. The ALS points were necessary because of the weak configuration of the images. Figure 2 shows an upright projection of a reference building resembling a hip roof and the ALS points. Three variants are shown: the results of photogrammetric plotting with and without geometric constraints and the results achieved by combining photogrammetric plotting with geometric constraints and ALS data. For the variant without geometric constraints the RMS values of the height differences of the horizontal eaves is ±0.25 m. In the constrained version, the eaves are horizontal, but the figure reveals that the heights of the eaves derived from the ALS data are about 50 cm lower. The ALS points were introduced as model co-ordinates; the shift was about 15 cm in X and Y and about 5 cm in Z. The precision of the building vertices was about ±17 cm in X and Y, and about ±5 cm in Z.

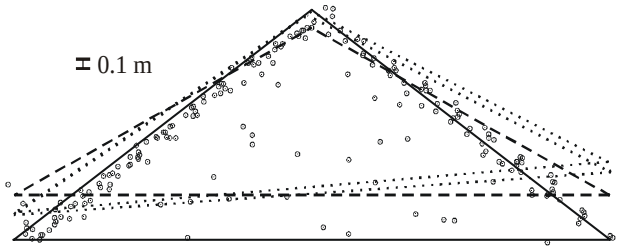

Figure 2. Upright projection of a hip roof (heights enlarged by a factor 2) generated from images without constraints (dotted lines); images with constraints (broken lines); images with constraints and ALS points (full lines). Circles: ALS points.

4.3 Results and Discussion

From the ALS data, a DSM with a grid width of Δ = 0.5 m was generated. From the DSM, roof planes were extracted, and the roof boundary polygons were determined as a combination of intersection lines and step edges in the way described in (Rottensteiner et al., 2005). These initial roof boundary polygons are shown super-imposed to the DSM in Figure 3.

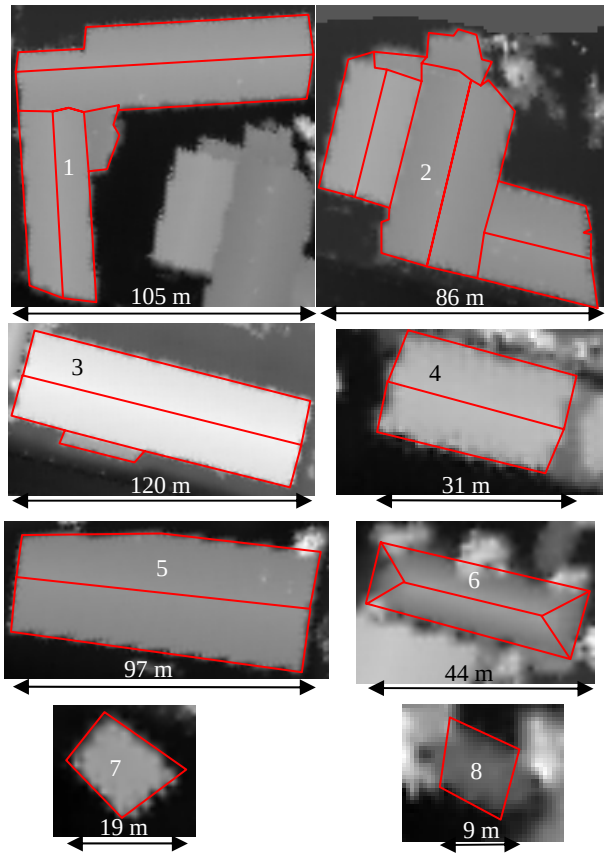

Figure 3. Initial roof boundary polygons for the eight buildings superimposed to the DSM. The buildings are shown in different scales, according to the extents shown in the figure.

In general the models look quite good except for building 8, which is partly occluded by trees. There is some noise in the outlines of buildings 1 and 2. Buildings 4, 6, 7, and 8 and the main part of building 3 should have a rectangular footprint, which is not entirely preserved in the initial models; geometric constraint should help to overcome this situation. The initial models, the original ALS points, and the step edge points provide the input for the overall adjustment. Soft constraints were introduced just on the basis of a comparison of angles/height differences to thresholds. Table 1 gives an overview about the stochastic model for the individual groups of observations in adjustment. Robust estimation was applied to the soft constraints and to the ALS and step edge points. In the current implementation this had to be done in a supervised way. It turned out that with some larger buildings the stochastic model had to be changed to make false hypotheses on geometric constraints detectable. Using σ_C = ±0.05 m and σ_E = ±0.25 m turned out to be a good choice. However, the final adjustment without the eliminated observations was carried out using the values given in Table 1. They were confirmed by a variance component analysis.

Topology σ_T [m]	Constraints σ_C [m]	ALS XY σ_{XY} [m]	ALS Z σ_Z [m]	Step Edge σ_E [m]
±0.01	±0.015	±0.25	±0.075	±0.5

Table 1. A priori standard deviations of the observations.

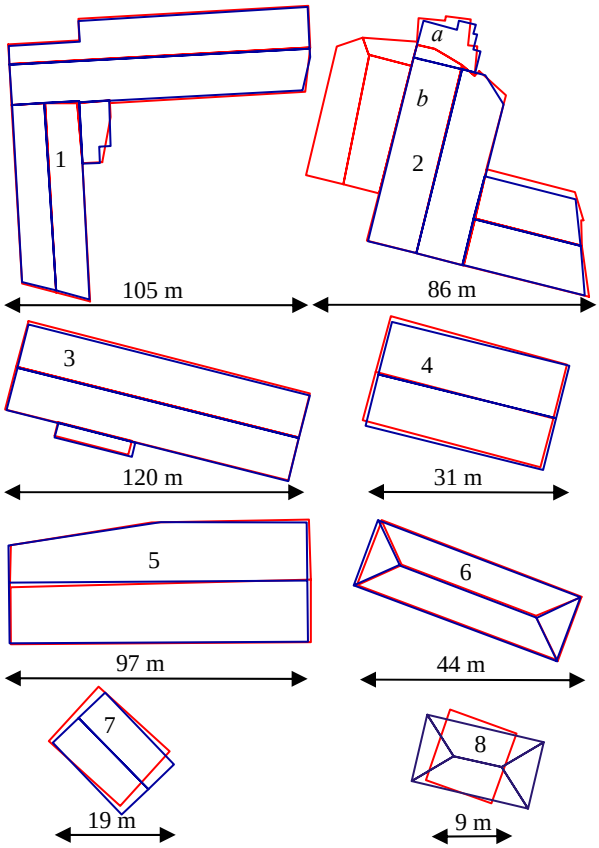

Figure 4. Final roof boundary polygons (red) and reference data (blue). A part of building 2 is missing in the reference data since it only occurs in the ALS data.

Figure 4 gives the final results of building reconstruction and a comparison to the reference data. Compared to figure 3, the building models appear to be more regular. For buildings 1-6 the number of extracted roof planes was correct. The intersection lines are very accurate, and step edges are in general determined quite well, too. Some small roof structures are generalised, e.g. the outline of the smallest roof plane of building 1 or of roof plane *a* of building 2. The step edge between that plane and its neighbouring plane *b* was also not very precisely determined. The problem was that roof plane *a* was horizontal, its western vertex being higher and its eastern vertex lower than the corresponding vertices of roof plane *b*; the maximum height difference was only 0.3 m, so that the step edge was poorly defined. Building 7 was reconstructed as being flat. The intersection of the two roof planes is only 0.15 m lower than the eaves, which is the reason why the two planes were merged. Building 8 was also reconstructed as a flat roof. It was the smallest building in the sample with only a few ALS points on the roof planes, and both ends occluded by trees. The outlines at the occluded ends are not very well detected either. Apart from the visual inspection of the building models, a numerical evaluation of these results was carried out. RMS values of the co-ordinate differences of corresponding vertices in the reconstruction results and the reference data were computed for each roof plane:

$$RMS_{XY} = \sqrt{\frac{\sum\left(\Delta X^2 + \Delta Y^2\right)}{N}} \text{ and } RMS_Z = \sqrt{\frac{\sum \Delta Z^2}{N}} \quad (3)$$

In Equation 3, N is the number of corresponding points in the respective roof plane. If no matching vertex was found, the closest point on the corresponding roof boundary polygon was used instead. For buildings 7 and 8 only the outlines were evaluated. Figure 5 shows a graph of RMS_{XY} and RMS_Z depending on the roof area. RMS_{XY} is smaller than 3.1 m for all roof planes. For most roofs it is in the range between ±0.5 m and ±1.5 m, which is better than the point density across the flight direction. The largest values occur for roof planes smaller than 100 m^2, with the exception of roof planes *a* and *b* of building 2, for reasons discussed above. RMS_Z is much smaller than RMS_{XY} because heights are better defined in ALS data than step edges. RMS_Z becomes smaller with increasing area roof planes because more ALS points give support to large planes. Intersections are more accurately determined than step edges. RMS values computed for intersection lines are only ±0.35 m in planimetry and ±0.07 m in height.

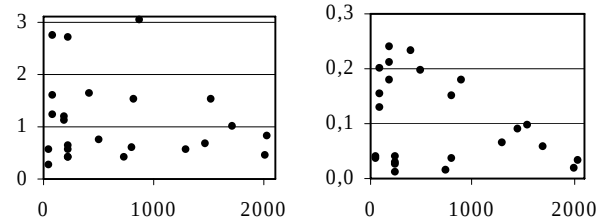

Figure 5. Left: RMS_{XY} [m], right: RMS_Z [m], both depending on the roof area [m^2].

B	*P*	RMS_{XY} [m]	RMS_Z [m]	Δ_{XY} [m]	Δ_Z [m]
1	5	0.76	0.12	0.24	0.01
2	5	2.27	0.20	0.00	-0.02
3	3	0.82	0.10	0.07	0.16
4	2	0.60	0.02	0.13	0.03
5	2	1.31	0.08	-0.08	-0.02
6	4	0.48	0.09	0.36	0.17
7	2	1.43	0.14	0.44	0.03
8	O	2.74	-	-0.02	-

Table 2. *B*: Building; *P*: Number of planes; RMS_{XY}, RMS_Z: Combined RMS values in planimetry / height; Δ_{XY}, Δ_Z: improvement of RMS_{XY} / RMS_Z.

Table 2 gives combined RMS values for all the test buildings. The large value for RMS_{XY} for building 2 of ±2.27 m is caused by the erroneous step edge; the combined value without that edge would be ±1.43 m. For most buildings, RMS_{XY} is better than the average point distance across flight direction. Apart from problems with low step edges, errors occurred at the outlines of some of the larger building due to occlusions: as the test area was at the edge of the swath, the positions of the step edges were very uncertain there. The height accuracy is good, with the largest value of ±0.20 m occurring at building 2, again at the problematic step edge. Table 2 also gives the impact of the overall adjustment to the RMS values. With building 5, the RMS values get worse by a small value after adjustment, but in most cases the RMS values are improved by the overall adjustment. The improvement can be up to 45% (building 6).

5. CONCLUSION

In this paper we have described a model for the consistent estimation of building parameters that is part of a method for the automatic reconstruction of buildings from ALS data. The adjustment model can consider geometric regularities by "soft constraints", and it can handle different sensor data. It was used not only in the reconstruction process, but also for the generation of reference data for a test project. In the test project, the roof boundary polygons extracted from the ALS data were compared to the reference data. The accuracy was determined to be in the range of or better than the average point distance in planimetry, and about ±0.1 - ±0.2 m in height. The improvement of the model co-ordinates caused by the geometric constraints can be up to 45 %.

ACKNOWLEDGEMENT

The data set used in this study was provided by AAM Hatch (www.aamhatch.com.au).

REFERENCES

Alharty, A., Bethel, J., 2004. Detailed building reconstruction from airborne laser data using a moving surface method. In: *IAPRSIS* XXXV - B3, pp. 213-218.

Ameri, B., 2000. Feature based model verification (FBMV): A new concept for hypotheses validation in building reconstruction. In: *IAPRS* XXXIII-B3A, pp. 24-35.

Brenner, C., 2000. Dreidimensionale Gebäuderekonstruktion aus digitalen Oberflächenmodellen und Grundrissen. PhD thesis, University of Stuttgart. DGK-C 530.

Brenner, C., 2005. Constraints for modelling complex objects. In: *IAPRSIS* XXXIII-3/W24, pp. 49 - 54.

Heuel, S., 2004. *Uncertain Projective Geometry. Statistical Reasoning for Polyhedral Object Reconstruction*. Springer-Verlag, Berlin Heidelberg, Germany.

Kager, H., 2000. Adjustment of Algebraic Surfaces by Least Squared Distances. In: *IAPRS,* Vol. XXXIII-B3, pp. 472–479.

McGlone, C., 1996. Bundle adjustment with geometric constraints for hypothesis evaluation. *IAPRS*, Vol. XXXI-B3, pp. 529–534.

Rottensteiner, F., 2003. Automatic generation of high-quality building models from Lidar data. *IEEE CG&A* 23(6), pp. 42-51.

Rottensteiner, F. and Schulze, M, 2003. Performance evaluation of a system for semi-automatic building extraction using adaptable primitives. In: *IAPRSIS* XXXIV / 3-W8, pp. 47-52.

Rottensteiner, F., Trinder, J., Clode, S., and Kubik, K., 2005. Automated delineation of roof planes in LIDAR data. In: *IAPRSIS XXXVI – 3/W19*, pp. 221-226.

Vallet, B., Taillandier, F., 2005. Fitting Constrained 3D Models in Multiple Aerial Images. In: *BMVC*, accessed 19/07/2006: http://www.bmva.ac.uk/bmvc/2005/papers/paper-57-176.html

Vögtle, T., Steinle, E., 2000. 3D modelling of buildings using laser scanning and spectral information. In: *IAPRS* XXXIII-B3B, pp. 927-933.

Vosselman, G., 1999. Building reconstruction using planar faces in very high density height data. In: *IAPRS* XXXII/3-2W5, pp. 87–92.